⌘ *Author's Choice*

THE JOURNAL OF BIOLOGICAL CHEMISTRY VOL. 285, NO. 26, pp. 20328–20342, June 25, 2010

AKAP79/150 Interacts with AC8 and Regulates Ca^{2+}-dependent cAMP Synthesis in Pancreatic and Neuronal Systems*[S]

Received for publication, March 5, 2010, and in revised form, April 21, 2010 Published, JBC Papers in Press, April 21, 2010, DOI 10.1074/jbc.M110.120725

Debbie Willoughby, Nanako Masada, Sebastian Wachten, Mario Pagano, Michelle L. Halls, Katy L. Everett, Antonio Ciruela, and Dermot M. F. Cooper[1]

From the Department of Pharmacology, University of Cambridge, Tennis Court Road, Cambridge CB2 1PD, United Kingdom

Protein kinase A anchoring proteins (AKAPs) provide the backbone for targeted multimolecular signaling complexes that serve to localize the activities of cAMP. Evidence is accumulating of direct associations between AKAPs and specific adenylyl cyclase (AC) isoforms to facilitate the actions of protein kinase A on cAMP production. It happens that some of the AC isoforms (AC1 and AC5/6) that bind specific AKAPs are regulated by submicromolar shifts in intracellular Ca^{2+}. However, whether AKAPs play a role in the control of AC activity by Ca^{2+} is unknown. Using a combination of co-immunoprecipitation and high resolution live cell imaging techniques, we reveal an association of the Ca^{2+}-stimulable AC8 with AKAP79/150 that limits the sensitivity of AC8 to intracellular Ca^{2+} events. This functional interaction between AKAP79/150 and AC8 was observed in HEK293 cells overexpressing the two signaling molecules. Similar findings were made in pancreatic insulin-secreting cells and cultured hippocampal neurons that endogenously express AKAP79/150 and AC8, which suggests important physiological implications for this protein-protein interaction with respect to Ca^{2+}-stimulated cAMP production.

Multimolecular signaling complexes organized around protein kinase A anchoring proteins (AKAPs)[2] provide a focal point for the activities of cAMP-dependent protein kinase (PKA) and other signaling molecules to produce spatially and temporally discrete cAMP-dependent events. Such localized action of cAMP is believed to account for the diverse physiological effects of this ubiquitous messenger within the cell (1, 2). The AKAPs form a large family of scaffold proteins that preferentially target PKA to discrete regions of the cell (*e.g.* plasma membrane, Golgi, or mitochondria) (1, 3). In addition, AKAPs associate with a range of other signaling proteins, including protein kinase C, Epac (exchange protein directly activated by cAMP), phosphatases (*e.g.* PP2B), and cAMP-dependent phosphodiesterases (*e.g.* PDE4) as well as a wide range of specific ion channel and receptor subtypes (1, 4).

Recent studies have revealed that specific adenylyl cyclase (AC) isoforms can also form an integral part of AKAP-based signaling complexes. In the first demonstration of this kind, AKAP79 was shown to directly interact with AC5 and AC6 to facilitate PKA-mediated inhibition of cAMP production (5). More recently, the plasma membrane-targeted AKAP, Yotiao (a splice variant of AKAP9), was found to directly interact with AC1 and AC2 (6). Interactions with Yotiao inhibited AC2 activity, but the functional consequence of the association between Yotiao and AC1 was not apparent. In a separate study, the muscle-specific AKAP, mAKAPβ, was found to interact with and inhibit the activity of AC5 to provide an additional role for mAKAPβ in the regulation of hypertrophy (7).

Further compartmentalization of cAMP signals within the cell is achieved by the Ca^{2+}-dependent regulation of specific AC isoforms. Activities of four of the nine membrane-bound AC isoforms are sensitive to submicromolar changes in local [Ca^{2+}]. AC1 and AC8 are stimulated by Ca^{2+}/calmodulin and, *in vivo*, are highly selective for Ca^{2+} increases arising from store-mediated Ca^{2+} entry or voltage-gated Ca^{2+} channel activity. AC5 and AC6 display similar selectivity for the source of Ca^{2+}-rise, but they are directly inhibited by Ca^{2+} (8). Previous work from our laboratory has shown that the largest, most dynamic changes in intracellular [cAMP] arise in subcellular domains close to sites of Ca^{2+} entry (9–11). Furthermore, cAMP levels can oscillate as a function of agonist-evoked intracellular Ca^{2+} transients (12–14). Interestingly, a number of the Ca^{2+}-regulated ACs are among those isoforms that are reported to interact with AKAPs (*e.g.* the interaction of Ca^{2+}-inhibitable AC5 with AKAP79 (5) or mAKAPβ (7) and interaction of Ca^{2+}-stimulated AC1 with Yotiao (6)). Nevertheless, the functional role of AKAP association with respect to Ca^{2+} regulation of the ACs has not been examined. Because these enzymes are predominantly regulated by local Ca^{2+} changes and a number of AKAP species have been shown to interact with Ca^{2+} regulatory proteins (*e.g.* L-type Ca^{2+} channels or inositol 1,4,5-trisphosphate receptor (15, 16)), an additional function of the AKAPs to localize specific AC isoforms, not

* This work was supported by Wellcome Trust Grant RG31760.
⌘ *Author's Choice*—Final version full access.
[S] The on-line version of this article (available at http://www.jbc.org) contains supplemental Fig. 1.
[1] A Royal Society Wolfson Research Fellow. To whom correspondence should be addressed. E-mail: dmfc2@cam.ac.uk.
[2] The abbreviations used are: AKAP, protein kinase A anchoring protein; AC, adenylyl cyclase; CCE, capacitative Ca^{2+} entry; CFP, cyan fluorescent protein; Ci/C-Epac2-camps, citrine/CFP-tagged Epac2-based fluorescent cAMP sensor; Epac2-camps, YFP/CFP-tagged Epac2-based fluorescent cAMP sensor; FRET, fluorescence resonance energy transfer; FRET^c, corrected FRET signal; FRETN^c, normalization of corrected FRET signal; FSK, forskolin; GST, glutathione *S*-transferase; IBMX, 3-isobutyl-1-methylxanthine; PKA, protein kinase A; shRNA, short hairpin RNA; Tg, thapsigargin; YFP, yellow fluorescent protein; HA, hemagglutinin.

only with their effector molecules but also with sites of Ca^{2+} entry, could be envisaged.

In the present study, we have investigated whether AC8, a well characterized Ca^{2+}-stimulable AC, interacts with an AKAP and if such an interaction might affect Ca^{2+}-dependent AC8 activity. Our initial screen using GST pull-down assays identified AKAP79 and its rodent orthologue AKAP150 as candidate binding partners for AC8. Using a combination of co-immunoprecipitation, FRET analysis of protein-protein interaction, live cell imaging with a high resolution cAMP biosensor, and selected knockdown of AKAP79/150 using shRNA, we were able to establish a defined role for AKAP79/150-AC8 interaction and the regulation of Ca^{2+}-stimulated cAMP production. The functional interaction was observed in HEK293 (human embryonic kidney) cells overexpressing AC8 and AKAP79/150 but also in pancreatic MIN6 (mouse pancreatic β-cell line) insulin-secreting cells and cultured hippocampal neurons that endogenously express AC8 and AKAP79/150. These data provide the first evidence that AC8 interacts with an AKAP and demonstrate a role for AKAP79/150 in the attenuation of Ca^{2+}-dependent AC8 activity *in vivo*.

EXPERIMENTAL PROCEDURES

AKAP18α-Myc-His and GFP-AKAP149 were gifts from Dr. Enno Klussmann (LMP, Berlin, Germany); Myc-Yotiao was a gift from Dr. Carmen Dessauer (University of Texas, Houston, TX); FLAG-sAKAP84 and FLAG-AKAP-Lbc were gifts from Dr. Hiroshi Ariga (Hokkaido University, Japan); HA-gravin was a gift from Dr. Craig Malbon (SUNY, Buffalo, NY); AKAP150, pSilencer vector, and shRNA AKAP79 were gifts from Prof. John Scott (University of Seattle); WAVE-2 was a gift from Dr. Marc Kirschner (Harvard University, Boston, MA); AKAP79-YFP and AKAP79-CFP were gifts from Dr. Marc Dell'Acqua (University of Colorado, Denver, CO), GST-Ezrin was a gift from Dr. Kjetil Tasken (University of Oslo, Norway); and Epac2-camps was a gift from Dr. Martin Lohse (Würzburg, Germany).

Untagged versions of AKAP150 and WAVE were C-terminally HA-tagged using donated plasmid DNAs as template and subcloned into pcDNA3.1. DNA fragments encoding C-terminally HA-tagged AKAP proteins were generated by PCR. Primer sequences for AKAP150-HA were 5′-GGCGGATCCACCATGAAAGAGTGCAGTGTCAAAATG (forward) and 5′-GGCTCTAGATCAAGCGTAATCTGGTACGTCGTATGGGTACTGGAACAGCGTATTTATTTGATTA (reverse), and primer sequences for WAVE-HA were 5′-GGCGGTACCACCATGCCGTTAGTAACGAGGAAC (forward) and 5′-GGCGGTACCACCATGCCGTTAGTAACGAGGAAC (reverse). AKAP79-HA was generated from AKAP79-YFP. Primer sequences were 5′-GGCGGATCCACCATGGAAACCACAATTTCAGAAATTC (forward) and 5′-GGCGAATTCAAGCGTAATCTGGTACGTCGTATGGGTACTGTAGAAGATTGTTTATTTTATTATC (reverse). pcDNA3.1 AKAP149-HA was generated using the primer sequences 5′-GGCGGATCCACCATGGCAATCCAGTTCCGTTCG (forward) and 5′-GGCGAATTCAAGCGTAATCTGGTACGTCGTATGGGTAAAGGCTTGTGTAGTAGCTGTCTA (reverse). Ezrin-HA was generated from GST-Ezrin using the primer sequences 5′-GGCAAGCTTCCACCATGCCGAAACCAATCAATGTCC (forward) and 5′-GGCGAATTCAAGCGTAATCTGGTACGTCGTATGGGTACAGGGCCTCGAACTCGTCG (reverse).

The generation of DNA fragments encoding GST-AC8 1–179 and GST-AC8 1106–1248 was described previously (17). cDNAs encoding the AC8 fragments 1–77, 73–179, and 582–703 were subcloned into pGEX4T-1 using the EcoRI and SalI (residues 1–77 and 582–703) or the EcoRI and XhoI (residues 73–179) restriction sites to produce GST-tagged proteins. For AC8 1–77, primers were 5′-CGGAATTCATGGAACTCTCGGATGTGCAC (forward) and 5′-ACGCGTCGACTTACGCGTGGTGGTTTGGTCC (reverse). For AC8 73–179, primers were 5′-CGCGAATTCCCAAACCACCACGCGCCG (forward) and 5′-GCGCTCGAGCTACTCCGATTTGCGCCTCTGG (reverse). For AC8 582–703, primers were 5′-GGAATTCGAGACCTATTTGATTAAGCAGC (forward) and 5′-ACGCGTCGACAGTGATAAACAGAAGAACG (reverse). AC8M1(Δ1–106) with a C-terminal HA tag was inserted into pcDNA3 using the KpnI and XbaI restriction sites. Primer sequences were 5′-GGGGTACCGCCACCATGCCGGAACGCAGCGGGAGCGGC (forward) and 5′-GCTCTAGATTATGGCAAATCGGATTTG (reverse).

The original Epac2-camps sensor containing the FRET pair CFP and YFP (18) was modified to generate Ci/C-Epac2-camps, in which the YFP was replaced with citrine. The DNA fragment encoding citrine was generated by PCR using plasmid 12150 DNA as template (19). Primer sequences were 5′-GGCAAGCTTCCACCATGGTGAGCAAGGGCGAGG (forward) and 5′-CGAATTCCTTGTACAGCTCGTCCATGC (reverse). The PCR fragment was then cloned into pcDNA Epac2-camps (YFP/CFP) and digested with HindIII and EcoRI to remove the original YFP sequence.

Cell Culture and Transfections—HEK293 cells (European Collection of Cell Cultures, Porton Down, UK) were grown in minimum essential medium supplemented with 10% (v/v) fetal bovine serum, 100 units/ml penicillin, 100 μg/ml streptomycin, and 2 mM L-glutamine. Mouse insulin-secreting MIN6 β-cells (a gift from Dr. Anders Tengholm (Uppsala, Sweden)) were cultured in Dulbecco's modified Eagle's medium containing 4500 mg/ml glucose, supplemented with 15% fetal bovine serum, 100 units/ml penicillin, 100 μg/ml streptomycin, 2 mM L-glutamine, and 50 μM 2-mercaptoethanol. All cells were maintained at 37 °C in a humidified atmosphere of 5% CO_2, 95% air.

To produce stably expressing HEK-AC8 cells, wild-type HEK293 cells were plated on 100-mm dishes at ~60% confluence 1 day prior to transfection with 2 μg of rat AC8, AC8-HA, or 8M1-HA cDNA using the Lipofectamine 2000 transfection method. Two days later, the culture medium was replaced with fresh medium containing 800 μg/ml G-418 disulfate (Formedium Ltd., Hunstanton, UK) to select transfected cells. After selection, cells were maintained in medium containing 400 μg/ml G-418. Stable AC8-expressing HEK293 cells were established from ~2 weeks following transfection.

For single cell cAMP measurements and micro-FRET experiments, MIN6, untransfected HEK293, or stable AC8 (HEK-AC8) cells were plated onto 25-mm poly-L-lysine-coated coverslips at ~60% confluence 24 h prior to transient transfection with 1 μg of total cDNA (0.5 μg each if transfecting two con-

structs (*e.g.* Epac2-camps and AKAP)), using the Lipofectamine 2000 method. For *in vitro* FRET measurements, 10 μg of Epac2-camps or Ci/C-Epac2-camps sensor was transfected into HEK293 cells in 150-mm dishes using Lipofectamine 2000. For GST pull-down and co-immunoprecipitation assays, cells were plated onto 100-mm dishes at ~40% confluence 1 day prior to the transient transfection with 2 μg of AKAP cDNA according to the calcium phosphate method as described previously (20). All experiments were carried out ~48 h post-transfection.

Preparation of Primary Cultured Hippocampal Neurons—Hippocampal neurons were cultured from newborn Wistar rats as described previously (21) except that the growth medium used was Neurobasal medium (Invitrogen) containing 2% B27 (Invitrogen), 5% fetal calf serum (PAA Laboratories, GmbH, Pasching, Austria), 1 mM L-glutamine, 35 mM glucose (Sigma), 100 units/ml penicillin, and 0.1 mg/ml streptomycin (Invitrogen). 2.4 μM cytosine arabinoside (Sigma) was added to cultures 2–4 days after plating to inhibit proliferation of non-neuronal cells. All cultures were plated on poly-D-lysine-coated 18-mm glass coverslips and maintained at 37 °C in a humidified atmosphere of 95% air and 5% CO_2. At 10–12 days *in vitro*, neurons were transfected with a Ci/C-Epac2-camps sensor using the Lipofectamine 2000 method of transfection. Transfected neurons were imaged 48 h later.

Lentiviral Knockdown of Endogenous AKAP150—For knockdown of endogenously expressed AKAP150 in primary cultured hippocampal neurons, shRNA AKAP150 lentiviral particles (Santa Cruz Biotechnology, Inc., Santa Cruz, CA) were added directly to cultured cells 72 h prior to experiments. For introduction of shRNA AKAP150 to cultured MIN6 cells, the culture medium was replaced with fresh complete Dulbecco's modified Eagle's medium containing Polybrene (Santa Cruz Biotechnology, Inc.) at a final concentration of 5 μg/ml. shRNA AKAP150 lentiviral particles were added for overnight incubation before replacing the medium once again with complete Dulbecco's modified Eagle's medium. Control scrambled shRNA lentiviral particles were used as a negative control (Santa Cruz Biotechnology, Inc.).

GST-Fragment Purification—Fusion proteins of GST and AC8 fragments were expressed in BL21 cells at 30 °C following induction with 0.1 mM isopropyl 1-thio-β-D-galactopyranoside. Cells were lysed by sonication (three times for 30 s at 7–10 watts) in lysis buffer (50 mM Tris, pH 8, 20% (w/v) sucrose, 10% (v/v) glycerol, 2 mM $MgCl_2$, 200 μM $Na_2S_2O_5$, 1 mM dithiothreitol, and protease inhibitors). Homogenates were centrifuged (27,000 × *g*, 4 °C, 15 min), and supernatant was passed through a glutathione-Sepharose 4B resin by chromatography and washed until no protein remained in the eluate (assessed by measurement of absorbance at 280 nm). An equal volume of phosphate-buffered saline to resin with 0.02% NaN_3 was added to create a 50% slurry.

GST Pull-down Assays—Confluent 100-mm dishes of HEK293 cells transiently expressing the AKAP of interest were lysed in GST-Fish buffer (10% (v/v) glycerol, 100 mM NaCl, 50 mM Tris, pH 7.4; supplemented with 0.5% Tween 20, 100 μM EGTA, 2 mM dithiothreitol, 1 mM phenylmethylsulfonyl fluoride, 1 mM benzamidine, protease inhibitors, 10 mM β-glycerophosphate, and 2 mM sodium orthovanadate) by rotating for 30 min at 4 °C, before centrifugation (16,000 × *g*, 4 °C, 15 min). The cell lysate was incubated with the appropriate GST-fragment for 4 h at 4 °C with rotation. GST-beads were washed twice in GST-Fish buffer, and bound proteins were eluted by adding an equivalent volume of 2× Laemmli buffer and boiled for 5 min prior to Western blot analysis.

Co-immunoprecipitation—HEK293 cells expressing AC8-HA or co-expressing AC8-HA and CFP or AKAP79-CFP or pancreatic MIN6 cells were washed with phosphate-buffered saline and lysed in $C_{12}E_9$ solubilization buffer (50 mM Tris, pH 7.4, 1 mM EDTA, 1 mM $MgCl_2$, 150 mM NaCl, 0.5% (v/v) $C_{12}E_9$, and protease inhibitors) by repeatedly passing the cell suspension through a 21-gauge needle. The crude cell lysate was then centrifuged (200 × *g*, 4 °C, 5 min) to remove cellular debris. Lysates were precleared with 20 μl of prewashed protein A/G Plus-agarose beads (50% slurry; Santa Cruz Biotechnology, Inc.) for 1 h at 4 °C, and beads were precipitated by brief centrifugation. The appropriate immunoprecipitating antibody (anti-AKAP150 antibody (Santa Cruz Biotechnology, Inc.), anti-AKAP79 antibody (Millipore, Watford, UK), or anti-HA antibody (Sigma)) or control preimmune serum (normal goat, rabbit, or mouse IgG, respectively) was added to the supernatant and rotated for 1 h at 4 °C. Prewashed protein A/G Plus-agarose bead slurry (60 μl) was then added to each tube, and samples were rotated for 2 h at 4 °C. Beads were washed three times in wash buffer containing 50 mM Tris, pH 7.4, 1 mM EDTA, 1 mM $MgCl_2$, 150 mM NaCl, 0.05% (v/v) $C_{12}E_9$, and protease inhibitors and once with 50 mM Tris, pH 7.4. Bound proteins were eluted by adding an equivalent volume of 2× Laemmli buffer and incubated at 37 °C for 30 min prior to Western blot analysis.

For immunoprecipitation using anti-HA affinity-agarose beads (Roche Applied Science), lysates from HEK293 cells expressing AC8-HA or 8M1-HA were prepared as described above in Nonidet P-40 solubilization buffer (50 mM Tris, pH 7.4, 1 mM EDTA, 150 mM NaCl, 0.3% (v/v) Nonidet P-40, and protease inhibitors). The cell lysates were rotated with 100 μl of prewashed bead slurry (50%) for 4 h at 4 °C. Beads were washed five times in Nonidet P-40 solubilization buffer, and proteins were eluted with Nonidet P-40 solubilization buffer supplemented with 1% (w/v) SDS. Laemmli buffer was added to the elution and incubated at 37 °C for 30 min prior to Western blot analysis.

Western Blot Analysis—Proteins were resolved using 8, 10, or 12% SDS-polyacrylamide gels. Separated proteins were then transferred to a supported nitrocellulose membrane. Nitrocellulose membranes were blocked in TBS (20 mM Tris, pH 7.5, 150 mM NaCl) containing 5% (w/v) skimmed milk, for 30 min, followed by three 10-min washes in TBS supplemented with 0.05% (v/v) Tween 20 (TTBS). Membranes were incubated overnight at 4 °C with anti-AC8 antibody (1:1,000; gift from Dr. James Cali (Madison, WI)); anti-HA antibody (1:5,000; Sigma), anti-GFP antibody (1:5,000; Sigma), anti-AKAP79 antibody (1:5,000; Millipore); anti-AKAP149 (1:2,000; BD Biosciences); anti-AKAP150 (1:800; Santa Cruz Biotechnology, Inc.); anti-Myc antibody (1:5,000; Santa Cruz Biotechnology, Inc.), anti-FLAG antibody (1:5,000; Stratagene), or anti-GST antibody (1:40,000; Sigma) in TTBS containing 1% (w/v) skimmed milk.

Membranes were washed (3 times for 10 min each) in TTBS and then incubated with goat anti-rabbit IgG conjugated to horseradish peroxidase (1:20,000; for anti-AC8 and anti-AKAP79 antibodies), donkey anti-goat IgG conjugated to horseradish peroxidase (1:5,000; for anti-AKAP150), or goat anti-mouse IgG conjugated to horseradish peroxidase (1:20,000; for anti-HA, anti-FLAG, anti-Myc, anti-GST, and anti-GFP antibodies) in TTBS containing 5% (w/v) skimmed milk for 1 h. Finally, the membrane was washed three times in TTBS (10 min) and once in TBS (10 min), visualized with ECL Plus reagent (GE Healthcare) according to the manufacturer's protocol, and exposed to film. Immunoreactive bands were quantified by densitometry using Image J.

Single Cell Ca^{2+} Measurements—HEK-AC8 cells, MIN6 cells, or cultured hippocampal neurons (previously plated onto 25- or 18-mm coverslips) were loaded with 4 μM Fura-2/AM and 0.02% Pluronic F-127 (Invitrogen) for 35 min at room temperature. For HEK-AC8 cell experiments, extracellular buffered saline contained 140 mM NaCl, 4 mM KCl, 1 mM $CaCl_2$, 0.2 mM $MgCl_2$, 11 mM D-glucose, 10 mM HEPES, pH 7.4. For MIN6 cell experiments, extracellular buffered saline contained 125 mM NaCl, 4.8 mM KCl, 1.3 mM $CaCl_2$, 1.2 mM $MgCl_2$, 3 mM D-glucose, and 25 mM HEPES, pH 7.4. For hippocampal experiments, extracellular buffered saline contained 140 mM NaCl, 5 mM KCl, 5 mM $NaHCO_3$, 2 mM $CaCl_2$, 1 mM $MgCl_2$, 5.5 mM D-glucose, 20 mM HEPES, 1 mM glycine, at pH 7.4. After loading, cells were washed several times and then imaged using an Andor Ixon+ EMCCD camera (Andor, Belfast, UK) and monochromator system (Cairn Research, Kent, UK) attached to a Nikon Eclipse TE2000-S microscope (×40 objective). Emission images (ET510/80M) at 340 and 380 nm excitation were collected at 1 Hz using MetaFluor software (Molecular Devices). For zero calcium buffers, the constituents were the same as for extracellular buffer, but $CaCl_2$ was omitted and replaced by 0.1 mM EGTA.

Epac2-camps FRET Measurements—Fluorescent imaging of Epac2-camps or Ci/C-Epac2-camps expressing HEK293 cells, MIN6 cells, or cultured hippocampal neurons was performed using an Andor Ixon+ EMCCD camera and an Optosplit (505DC) to separate CFP (470 nm) and YFP/citrine (535 nm) emission images (Cairn Research, Kent, UK). For dual emission ratio imaging, cells were excited at 435 nm using a monochromator (Cairn Research) and 51017 filter set (Chroma Technology Corp.) attached to a Nikon eclipse TE2000-S microscope (×40 oil immersion objective). Emission images at 470 and 535 nm were collected every 3 s (250 ms integration time) and analyzed using Metamorph imaging software (Molecular Devices). Cells in which the CFP and YFP/citrine fluorescence intensity was less than twice the background signal were excluded, as were cells with excessive expression of the fluorescent probe. Single cell FRET data were plotted as changes in background-subtracted 470 nm *versus* 535 nm (CFP/YFP or CFP/citrine) emission ratio relative to maximum FRET ratio change seen with saturating cAMP concentrations.

Micro-FRET Analysis of Protein-Protein Interactions—All FRET images were collected with YFP- and CFP-tagged constructs using an Andor Ixon+ EMCCD camera and an Optosplit (505DC) to separate CFP (470 nm) and YFP (535 nm) emission images. Images were acquired and analyzed according to the three-cube micro-FRET method (22). In brief, a series of live cell images were first collected from cells expressing tagged or untagged CFP or YFP alone (300 ms integration time, 2 × 2 binning) to calculate values for CFP bleed-through into the YFP channel (63%) and YFP cross-excitation of CFP (5.7%) for our imaging system. To calculate FRET in cells co-expressing CFP- and YFP-tagged constructs of interest, three separate live cell images were obtained: (i) 435 nm excitation/470 nm emission (CFP image), (ii) 500 nm excitation/535 nm emission (YFP image), and (iii) 435 nm excitation/535 nm emission (uncorrected CFP/YFP FRET image). All images were then background-subtracted. To correct for CFP bleed-through and cross-excitation of YFP, 63% of the CFP image and 5.7% of the YFP image were subtracted from the CFP/YFP FRET image to produce a corrected pseudocolor FRET image, $FRET^c$. As well as examination of the AC8 and AKAP tagged constructs and the PKA-RII and AKAP tagged constructs, negative controls were performed in HEK293 cells expressing untagged CFP and YFP alone. In these cells, no $FRET^c$ signal was seen following fractional subtraction of the CFP and YFP images from the uncorrected FRET signal.

To quantify the degree of sensitized FRET seen between different pairings of CFP- and YFP-tagged constructs, average intensities of the $FRET^c$ images were divided by the product of the CFP and YFP image intensities to produce normalized $FRETN^c$ values (22).

In Vitro FRET Measurements—HEK293 cells transiently expressing Epac2-camps and Ci/C-Epac2-camps were washed twice with ice-cold phosphate-buffered saline, scraped from the dishes, and centrifuged at 200 × *g* for 5 min (room temperature). Cell pellets were resuspended in 5 mM Tris-HCl, 2 mM EDTA (pH 7.3) and lysed by repeatedly passing through a 21-gauge needle. Lysates were centrifuged at 20,000 × *g*, 4 °C for 1 h, and subsequently the fluorescence emission spectra of the supernatants were measured (excitation at 436 ± 8 nm, emission from 450 to 550 nm) in a PerkinElmer Life Sciences LS50B spectrofluorometer. Concentrations of cAMP were spectrofluorometrically established at $\lambda_{259\ nm}$, and sigmoidal dose-response curves were obtained using GraphPad Prism version 4 (GraphPad Software Inc., La Jolla, CA). Spectra were also obtained from Epac2-camps or Ci/C-Epac2-camps lysate at pH 6.7 to examine the effects of acidification on FRET signal.

Statistical Analysis—Unless stated otherwise, data were analyzed by one-way analysis of variance followed by Newman-Keuls multiple comparison tests using GraphPad Prism software. Data are presented as means ± S.E., with significance set at $p < 0.05$.

RESULTS

AKAP79/150 Associates with the N Terminus of AC8—To probe for potential interactions between the Ca^{2+}-stimulated AC8 and AKAPs, a number of HA-, Myc-, or FLAG-tagged AKAPs were transiently overexpressed in HEK293 cells and screened by GST pull-down assays (Fig. 1). Three cytosolic regions of AC8 were chosen as possible binding sites because these regions are highly divergent in length and sequence between ACs and could be expected to provide isoform-specific

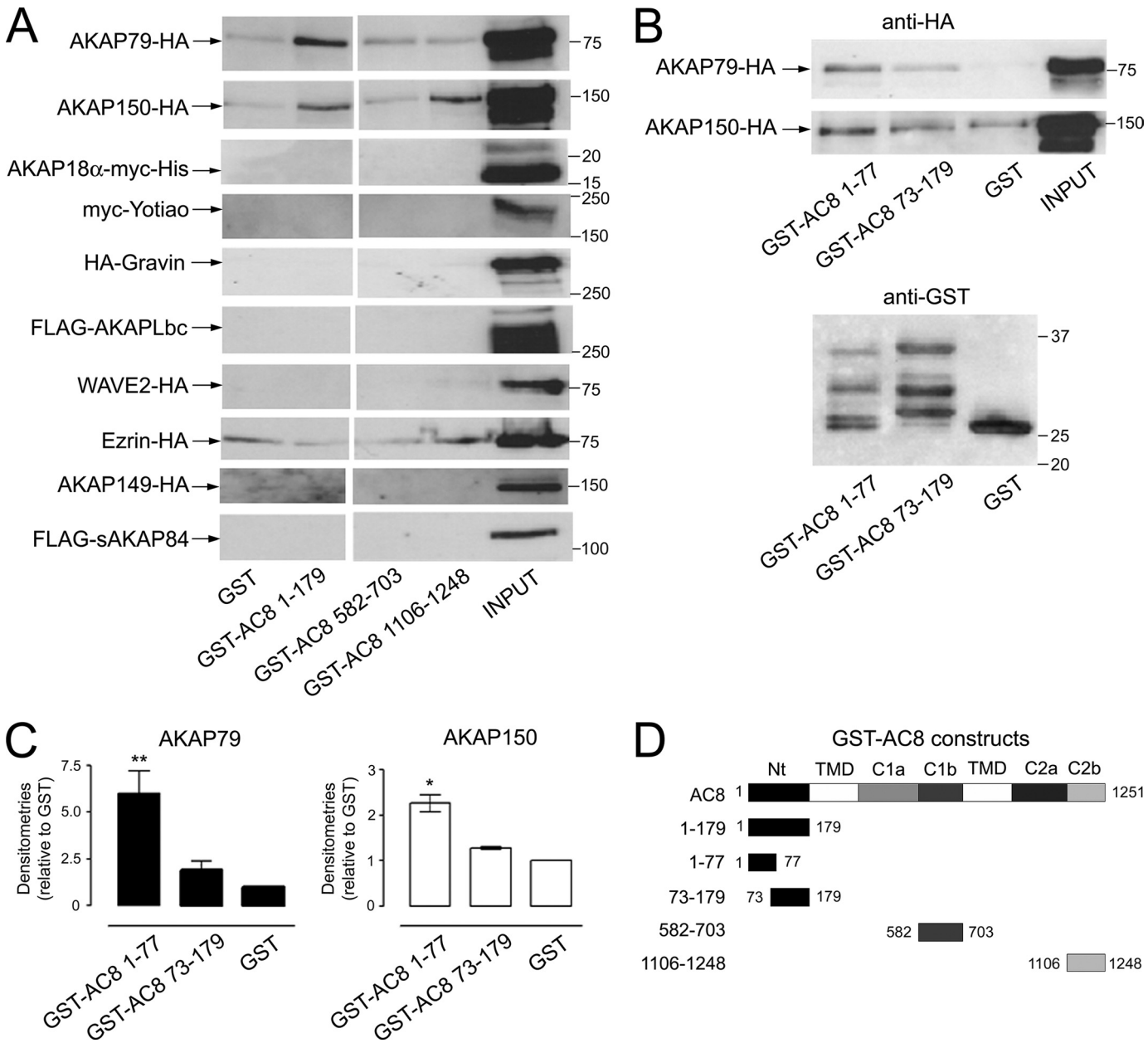

FIGURE 1. **Binding between AKAP79/AKAP150 and the N terminus of AC8.** *A*, GST pull-downs using whole cell lysate from cells transiently expressing tagged AKAP proteins. *Lane 1*, GST alone; *lanes 2–4*, the following regions of AC8 fused to GST: 1–179 (N terminus), 582–703 (C1b domain), and 1106–1248 (C terminus), respectively. *Lane 5*, input control (5%) to confirm expression of each construct. *B*, *top*, AKAP79-HA and AKAP150-HA transiently expressed in HEK293 cells were pulled down using GST-fused first half (residues 1–77) or second half (residues 73–179) of the AC8 N terminus. *Bottom*, immunoblotting of the GST-fused proteins used in the pull-downs in the *top*. The upper GST bands represent the full-length form of each protein. *C*, plot of densitometries from 3–6 repeats of blots presented in *B* to quantify binding of AKAP79/150 to GST-AC8 1–77 *versus* GST-AC8 73–179. Data are normalized to the intensity of the uppermost GST bands. *Error bars*, S.E. *D*, schematic diagram of GST-AC8 constructs used in *A–C*.

interactions with other proteins. Comparisons were made for the interaction of each AKAP with GST alone (*lane 1*) or with GST fused to the N terminus of AC8 (comprising residues 1–179; *lane 2*), the cytosolic C1b domain of AC8 (residues 582–703; *lane 3*), and the C terminus of AC8 (residues 1106–1248; *lane 4*). Immunoreactivities were then assessed using primary antibodies raised against the relevant AKAP fusion tag (HA, Myc, or FLAG). These Western blot analyses provided evidence of association between the N terminus of AC8 and both human AKAP79-HA and its rat orthologue AKAP150-HA (Fig. 1*A*, *lane 2*). A band was also present in *lane 2* of the Ezrin-HA blot; however, this appeared to be due to nonspecific interactions with GST alone (see Fig. 1*A*, *lane 1*). Interestingly, AKAP150-HA was also shown to interact with the C terminus of AC8 (Fig. 1*A*, *lane 4*), although there was no evidence of AKAP79-HA interaction with this domain, suggesting differences in the specific interactions between these two AKAP orthologues and AC8. Full-length AKAP79 and AKAP150 orthologues contain 427 amino acids and 1417 amino acids, respectively (23, 24). These two AKAPs share similar primary sequence and function; however, AKAP150 also contains multiple octapeptide sequence repeats of unknown function (23). It is possible

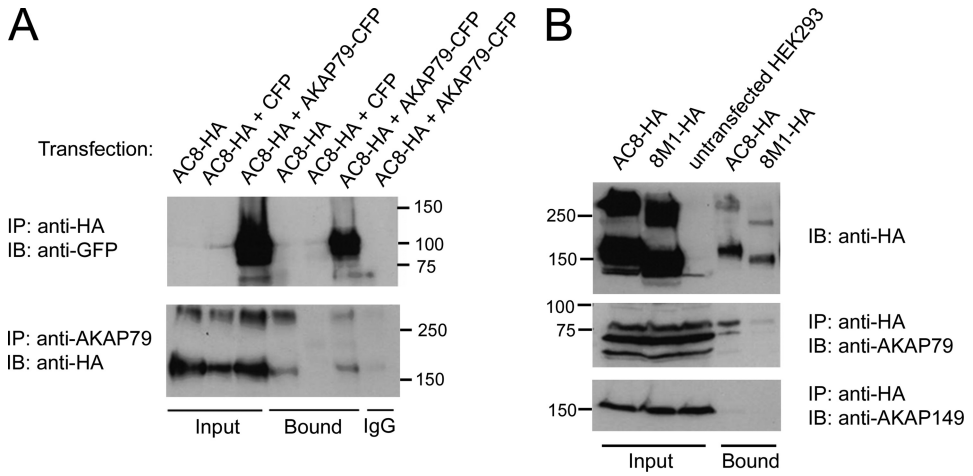

FIGURE 2. **Co-immunoprecipitation of AC8 and AKAP79 from HEK293 cell lysate.** *A*, *top blot*, AC8-HA immune complexes probed for AKAP79-CFP interaction using a GFP-specific antibody. The band at ~100 kDa in *lane 6* (bound fraction) provides evidence of interaction between AKAP79-CFP and AC8-HA. *Bottom blot*, reverse co-immunoprecipitation data in which cell lysates were immunoprecipitated (*IP*) with anti-AKAP79 antibody and Western blot analysis (*IB*) was with anti-HA antibody. Bands of ~170 kDa in *lanes 4* and *6* suggest interaction of AC8-HA with endogenous AKAP79 and overexpressed AKAP79-CFP, respectively. Input control (5%) is shown in *lanes 1–3*. *B*, co-immunoprecipitation of stably expressed AC8-HA or 8M1-HA with endogenous AKAP79 in HEK293 cells using HA-agarose beads. *Top blot*, confirms presence of AC8-HA and 8M1-HA (N-terminally truncated AC8) in HEK293 cell lysate fractions bound to HA-agarose beads. The *middle blot* was probed for the presence of AKAP79. A clear band is seen at ~75 kDa in the AC8-HA-bound fraction, providing evidence of interaction with AC8-HA. Little or no interaction was seen with the 8M1-HA. *Bottom blot*, as a negative control, fractions were also probed for AKAP149. Positive bands for AKAP149 were seen at ~150 kDa in *lanes 1–3* (5% input). No AKAP149 was detected in the bound fractions (*lanes 4* and *5*).

that the octapeptide repeats form an additional site of interaction with AC8 when overexpressed in HEK293 cells. AKAP18α-Myc-His, Myc-Yotiao, HA-gravin, FLAG-AKAP-Lbc, WAVE-HA, AKAP149-HA, and FLAG-sAKAP84 showed no sign of interaction with any of the GST-tagged regions of AC8 (Fig. 1*A*).

Having identified AKAP79 and AKAP150 as potential binding partners for the N terminus of AC8, further experiments were performed to narrow down the site of interaction between the AC and scaffold proteins (Fig. 1, *B* and *C*). GST pull-down assays were performed on whole cell lysates from HEK293 cells expressing AKAP79-HA or AKAP150-HA to compare the interaction of the two AKAP orthologues with the first half of the N terminus of AC8 (amino acids 1–77 of AC8 fused to GST) and the second half of the N-terminal region (amino acids 73–179 of AC8 fused to GST) (Fig. 1*B*). The GST pull-downs revealed that interaction between either AKAP79 or AKAP150 and AC8 occurred within the first 77 amino acids of the N terminus of AC8 (Fig. 1*B*) with little or no AKAP association with GST-AC8 73–179. Quantitation of the densitometries of HA-specific bands relative to GST signals revealed a 3.1-fold greater interaction by GST-AC8 1–77 compared with GST-AC8 73–179 with AKAP79 (Fig. 1*C*). For AKAP150, GST-AC8 1–77 bound with 1.6-fold greater efficiency than GST-AC8 73–179. This region of AC8 has previously been found to contain a helical calmodulin binding domain of AC8 (between residues 34 and 51) (25) and a binding site for protein phosphatase 2A that overlaps with the calmodulin binding domain (17).

Co-immunoprecipitation of Full-length AC8 and AKAP79 in HEK293 Cells—We next examined whether AKAP79 could interact with full-length, functional AC8 or a truncated form of AC8 (8M1), lacking the apparently critical first 106 residues, when co-expressed in HEK293 cells. AC8-HA immune complexes immunoprecipitated from HEK293 cell lysates were tested for interaction with AKAP79-CFP by Western blot using mouse anti-GFP antibody (Fig. 2*A*, *top blot*). Co-purification of AKAP79-CFP with AC8-HA was confirmed by the presence of a band at ~110kDa in *lane 6*, with no band detected in the IgG control (*lane 7*). A reverse co-immunoprecipitation experiment provided supporting evidence for the interaction of AC8-HA and AKAP79-CFP in HEK293 cell lysate (Fig. 2*A*, *bottom blot*). AKAP79-CFP immune complexes were immunoprecipitated using an AKAP79-specific antibody and probed for interaction with AC8-HA. The presence of an HA-specific band of ~170 kDa in *lane 6* confirmed co-purification of AC8-HA with AKAP79-CFP. The higher molecular weight band seen near the top of the blot corresponds to AC8 dimers (26, 27) and suggests that AKAP79 may also interact with higher orders of AC8 organization. Evidence of co-immunoprecipitation of AC8-HA with AKAP79 immune complexes in cells expressing AC8-HA alone (*lane 4*) was consistent with the interaction of AC8-HA with endogenous AKAP79 in HEK293 cells. Previous work from our laboratory has shown that AKAP79 is one of the major membrane-bound AKAP isoforms endogenously expressed in HEK293 cells (28).

To determine whether the N terminus of AC8 is indeed required for the interaction with AKAP79, similar co-immunoprecipitations were performed using lysate of HEK293 cells expressing either AC8-HA or the N-terminally truncated AC8 mutant, 8M1-HA (Δ1–106), with anti-HA affinity-agarose beads (Fig. 2*B*). The *top blot* confirmed the presence of AC8-HA (~170 kDa, *lane 4*) and 8M1-HA (~150 kDa, *lane 5*) in bound fractions. Blotting of the immune complexes with an AKAP79-specific antibody revealed interaction of AC8-HA with endogenously expressed AKAP79 (*middle blot*, *lane 4*). In contrast, 8M1-HA did not co-immunoprecipitate with AKAP79 (*middle blot*, *lane 5*). These results were in good agreement with the findings from Fig. 1, which suggested that the N terminus of AC8 (absent in 8M1) provides the site for interaction with AKAP79. Consistent with GST pull-down data (Fig. 1*A*), no band corresponding to the predicted molecular mass of AKAP149 (~150 kDa) could be seen in the AC8-HA-bound fraction (Fig. 2*B*, *bottom blot*, *lane 4*), showing no non-specific binding of AKAPs to the beads and confirming the specific interaction between AKAP79 and AC8.

Regulation of AC8 Activity by AKAP79 and AKAP150 in HEK293 Cells—The 10 AKAP isoforms used in our initial GST pull-downs to identify potential binding partners for AC8 (Fig.

1*A*) were examined in parallel studies to see if their expression evoked any functional effects on AC8 activity. Capacitative Ca^{2+} entry (CCE) was induced in intact HEK293 cells to isolate AC8-dependent cAMP production from that mediated by endogenously expressed (Ca^{2+}-insensitive) ACs. Previous studies have shown that Ca^{2+}-dependent stimulation of AC8 activity is highly selective for store-operated, or capacitative, Ca^{2+} entry over other modes of Ca^{2+} rise in non-excitable cells (10). Thus, HEK-AC8 cells expressing the Epac2-camps FRET-based biosensor for cAMP (18) were pretreated with the sarco-/endoplasmic reticulum Ca^{2+}-ATPase pump inhibitor, thapsigargin (Tg; 200 nM) in the absence of external Ca^{2+}. This enabled passive depletion of the endoplasmic reticulum Ca^{2+} stores, priming the system for sustained store-operated Ca^{2+} entry upon the addition of 2 mM external Ca^{2+} to the bath solution (as measured using Fura-2; Fig. 3*B*).

Measurements from HEK-AC8 cells expressing Epac2-camps were used to quantitate the effects of transient AKAP expression on CCE-induced AC8 activity (Fig. 3, *A* and *C*). *Pseudocolor images* presented in Fig. 3*D* represent typical FRET ratio changes evoked by CCE in control cells expressing the cAMP biosensor. The switch to warmer colors at 400 s (during CCE) compared with the FRET ratio at rest (200 s) indicated an increase in cAMP levels as a consequence of enhanced AC8 activity. Expression of AKAP79-HA attenuated the peak response of AC8 to CCE by around 20% ($p < 0.01$ compared with control) and suggested that the interaction between the N termini of AKAP79 and AC8 (Fig. 1) played an important role in the regulation of AC8 by Ca^{2+}. Interestingly, expression of AKAP150-HA potentiated the degree of Ca^{2+}-stimulated AC8 activity ($p < 0.05$). At present, the reason for opposing effects of the human AKAP79 and the rat AKAP150 orthologues with respect to AC8 activity in HEK293 cells is unclear. However, the additional association of the C terminus of AC8 with AKAP150, not seen with AKAP79, could be linked to different functional effects of the two AKAPs (Fig. 1*A*, *lane 4*). Despite showing no signs of direct interaction, based on our GST pull-down data, three other AKAPs appeared to significantly up- or down-regulate AC8 activity. Expression of plasma membrane-targeted AKAP18α-Myc-His (also known as AKAP15) reduced AC8 activity but to a lesser extent than that seen with AKAP79 expression ($p < 0.05$). Furthermore, an enhancement of CCE-mediated AC8 activity was seen following expression of the membrane-associated AKAP Myc-Yotiao ($p < 0.05$), and the mitochondrially targeted AKAP149-HA produced a more robust potentiation of AC8 activity ($p < 0.01$) (Fig. 3, *A* and *C*). In summary, the most potent effects on CCE-induced AC8 activity were seen with AKAP79-HA, AKAP150-HA, and AKAP149-HA. Because AKAP149-HA and the other two AKAPs, Myc-Yotiao and AKAP18α-Myc-His, did not appear to interact directly with AC8 (Figs. 1*A* and 2*B*), their effects on AC8 activity were not investigated further.

We considered the possibility that the maximal effects of AKAP79-HA expression on AC8 activity were curtailed due to high levels of endogenous AKAP79 in HEK293 cells (supplemental Fig. 1*A*) (28). To further examine the potential of AKAP79 and AC8 interaction, HEK-AC8 cells were treated with an shRNA directed against AKAP79. This shRNA depleted endogenous AKAP79 levels in HEK293 cells by more than 80% in our hands (supplemental Fig. 1*A*). Around 72 h following shRNA AKAP79 plasmid transfection, Ca^{2+}-stimulated AC activity in HEK-AC8 cells was significantly increased, by around 30% ($p < 0.001$; Fig. 4, *A* and *D*). The peak rate of signal rise was also enhanced to 2.5 times that seen under control conditions ($p < 0.001$; Fig. 4*D*). Fura-2 experiments were carried out to examine whether the effects of AKAP79 knockdown (Fig. 4, *A* and *D*) or the effects of overexpression of AKAP79-HA (Fig. 3*C*) or AKAP150-HA (Fig. 3*C*) on AC8 activity were an indirect consequence of altered CCE under these conditions. Measurements of intracellular Ca^{2+} changes showed comparable Ca^{2+} entry upon the addition of 2 mM extracellular Ca^{2+} to store-depleted cells under all four transfection conditions (Fig. 4*B*), indicating more direct effects of the AKAPs on Ca^{2+}-regulated AC8 activity.

To further validate a specific role for AKAPs in the control of Ca^{2+}-stimulated AC8 activity, the effects of the AKAP disruptor peptide, St-Ht31, were examined. Pretreatment of HEK-AC8 cells with 10 μM St-Ht31 for 40 min significantly enhanced CCE-mediated AC8 activity ($p < 0.001$; Fig. 4, *C* and *D*), and this enhancement was comparable with the effects of AKAP79 knockdown (Fig. 4*A*). The negative control peptide, St-Ht31P, was without effect (Fig. 4, *C* and *D*).

Imaging the AKAP79 and AC8 Interaction in Live Cells—Biochemical studies using GST pull-downs and co-immunoprecipitation in whole cell lysate have provided evidence for an association between the N termini of AKAP79 and AC8 (Figs. 1 and 2). Here, we have used "micro-FRET" to examine this protein-protein interaction at the single cell level in HEK293 cells expressing YFP- and CFP-tagged AC8 and AKAP79 constructs (Fig. 5). This technique takes into account variable CFP and YFP expression in transient transfections to provide a high resolution measurement of sensitized FRET, which is corrected for any potential bleed-through in fluorescence signals in the YFP and CFP emission images (22). Using micro-FRET, we were able to demonstrate a protein-protein interaction between YFP-AC8 and AKAP79-CFP. The degree of FRET seen at the plasma membrane was enhanced when we co-expressed 8Tm1/YFP/Tm2 with AKAP79-CFP. 8Tm1/YFP/Tm2 is a truncated version of AC8 in which YFP has been inserted between residues 1–397 and residues 654–956 (26). Importantly, this AC8 construct contains the full-length N terminus of AC8 but lacks most of the cytosolic C1 and C2 domains. Quantification of the FRET signal was achieved by normalization of the corrected FRET image ($FRETN^c$; see "Experimental Procedures") and indicated 70% greater $FRETN^C$ when 8Tm1/YFP/Tm2 was used instead of YFP-AC8 (Fig. 5, *bar chart*). The average $FRETN^c$ value of 10.8 ± 2.1 for 8Tm1/YFP/Tm2 and AKAP79-CFP interaction was comparable with our positive control, which used AKAP79-YFP and PKA-RIIα-CFP binding to provide a $FRETN^c$ value of 13.4 ± 3.4. This latter value is consistent with previous micro-FRET studies examining the interaction between PKA and its scaffold protein (29). The ability of 8Tm1/YFP/Tm2 to bind AKAP79 further supports the importance to the interaction of the N terminus of AC8 and the insignificance of the C1 and C2 domains. Negative controls in cells that co-expressed both AKAP79-YFP and

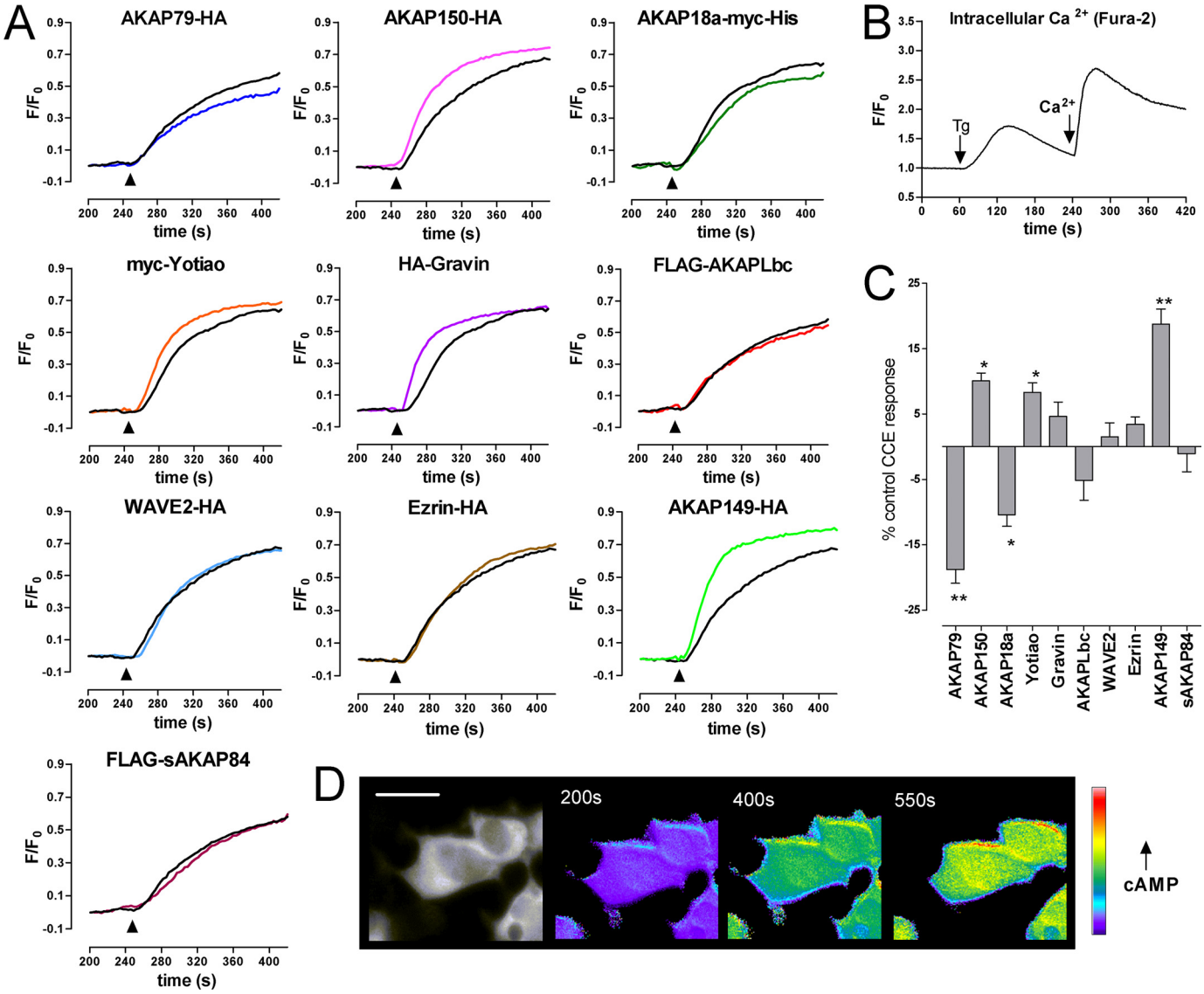

FIGURE 3. **Screening of the effects of AKAP expression on Ca^{2+}-stimulated AC8 activity.** *A*, CCE-mediated increases in cAMP production in HEK-AC8 cells assessed using the FRET-based sensor Epac2-camps. Data are plotted as relative FRET ratio changes with F_0 taken at 200 s, and F/F_0 is then normalized to the maximum signal response seen following stimulation with a mixture containing 10 μM FSK, 10 μM isoproterenol, 10 μM prostaglandin E_1, and 100 μM IBMX. *B*, average Fura-2 trace showing cytosolic Ca^{2+} changes in HEK-AC8 cells ($n = 100$ cells) during 200 nM Tg-induced store depletion in the absence of external calcium and subsequent CCE upon the addition of 2 mM Ca^{2+} to the bath solution. *C*, data analyses showing mean ± S.E. (*error bars*) of peak response to CCE in cells expressing the tagged AKAPs, compared with that seen under control conditions. *n* values range from 22 to 38 cells. *, $p < 0.05$; **, $p < 0.01$. *D*, *monochrome image* shows YFP signal (500 nm emission, 535 nm excitation) in HEK-AC8 cells expressing the Epac2-camps sensor. *Scale bar*, 20 μm. The *pseudocolor images* represent the FRET ratio at various time points during control experiments, with warmer colors (*green/yellow*) indicating higher cAMP levels. The *image* at 200 s is representative of basal cAMP, 400 s represents response to CCE, and 550 s represents maximal FRET signal seen in response to saturating cAMP levels.

AKAP79-CFP or untagged CFP and YFP demonstrated good co-localization but, as expected, no FRET signal.

Evidence of an Endogenous AC8 and AKAP150 Interaction in MIN6 Cells—Having proven that AC8 and AKAP79/150 can interact in HEK293 cells overexpressing tagged versions of AC8 and AKAP79/150, we sought to establish whether a similar interaction could be detected in a more physiological system in which both proteins are expressed endogenously. A recent study by our laboratory demonstrated the presence of Ca^{2+}-stimulable AC8 activity in a mouse insulin-secreting pancreatic β-cell line, MIN6 (30). Here, the endogenous expression of the rodent AKAP79 orthologue, AKAP150, in MIN6 cells was confirmed by Western blot analysis (Fig. 6*A*, *left*). This AKAP150-specific band was absent in HEK293 cells stably expressing AC8. Using an AC8-specific antibody, we also confirmed the presence of AC8 (band ~170 kDa) but at far lower levels than those seen when AC8 is overexpressed in HEK293 cells (Fig. 6*A*, *right*). Using the AKAP150-specific antibody to immunoprecipitate endogenous AKAP150 from MIN6 cell lysates, we could demonstrate the interaction with endogenously expressed AC8 (Fig. 6*B*, *lane 2*) but not with the IgG control (*lane 1*).

Functional Consequences of an AC8 and AKAP150 Interaction in Endogenously Expressing Systems—To establish whether the AC8-AKAP150 signaling complex plays an important functional role in the regulation of AC8 in MIN6 cells, we

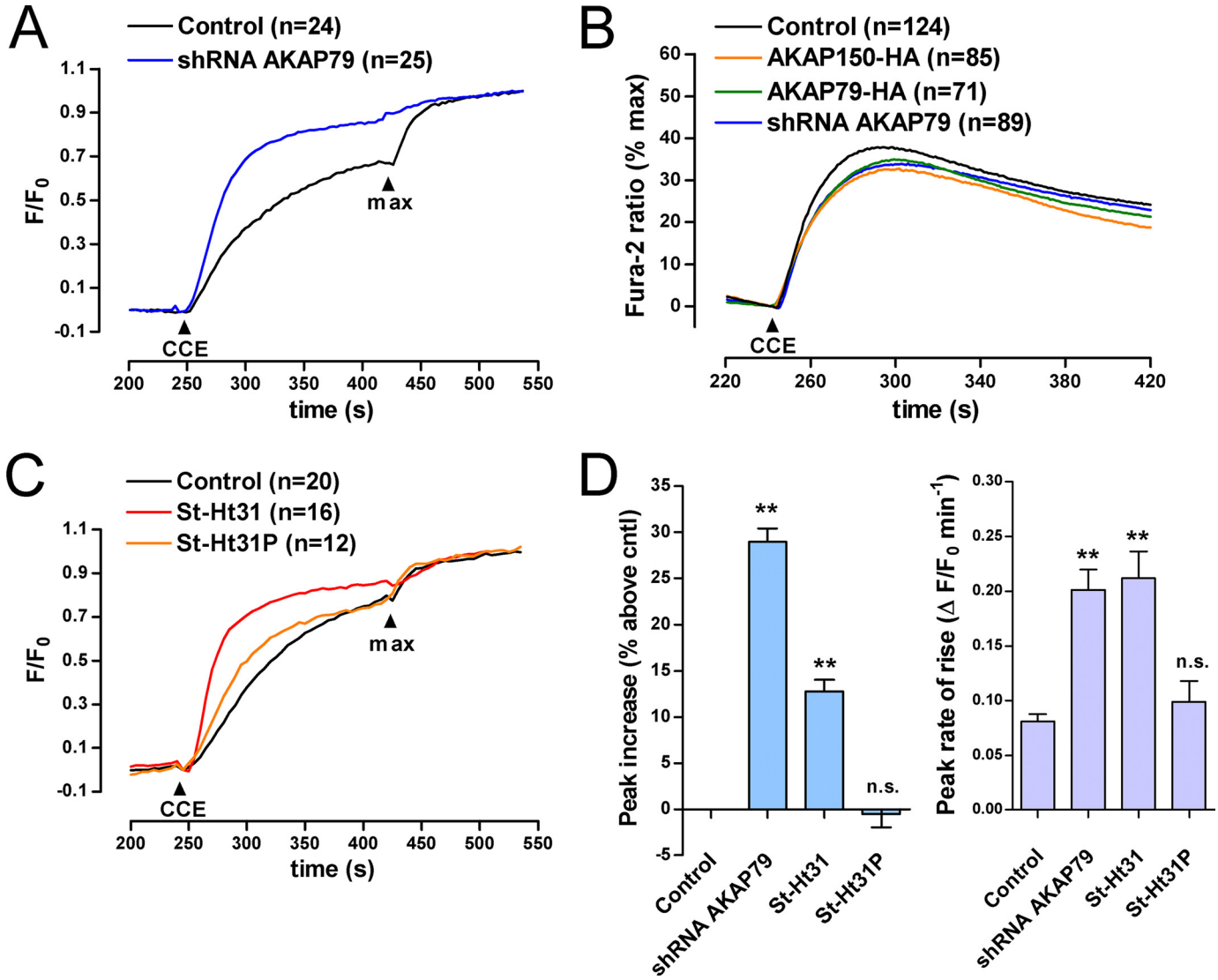

FIGURE 4. **AKAP disruption enhances CCE-induced AC8 activity.** *A*, CCE-mediated increases in cAMP assessed using the FRET-based sensor Epac2-camps following knockdown of endogenous AKAP79 levels. Data are plotted as relative FRET ratio changes normalized to maximum signal response. Cells were pretreated with 200 nM Tg in Ca^{2+}-free conditions, and CCE was induced upon the addition of 2 mM Ca^{2+} to the bath solution. *B*, average Fura-2 traces from HEK-AC8 cells during CCE following transfection with AKAP150-HA, AKAP79-HA, or shRNA AKAP79. All data are normalized to maximal Fura-2 signal obtained upon the addition of 5 μM ionomycin (Ca^{2+} ionophore) and 5 mM Ca^{2+}. *C*, effects of the AKAP/PKA disruptor peptide, St-Ht31 (10 μM), on CCE-stimulated AC8 activity assessed using Epac2-camps. Experiments were performed in the presence of 100 μM IBMX, and CCE was induced upon the addition of 0.5 mM Ca^{2+}. St-Ht31P (10 μM) was used as a negative control. *D*, analyses of the effects of AKAP79 knockdown or pharmacological AKAP disruption (St-Ht31) on AC8 activity. Plots of peak CCE-induced cAMP increase relative to control (*left chart*) and peak rate of cAMP production (*right chart*) are presented as mean ± S.E. (*error bars*). **, $p < 0.001$ using Students' *t* test.

assessed the consequences of AKAP150 knockdown and overexpression on CCE-induced AC8 activity (Fig. 7). Because MIN6 cells express both AC8 and the Ca^{2+}-inhibitable AC6, conditions were optimized for stimulation rather than inhibition of AC activity by using 2 mM extracellular Ca^{2+} to trigger CCE. Higher Ca^{2+} concentrations have been shown to preferentially influence Ca^{2+}-inhibitable AC6 activity (30). Store-mediated Ca^{2+} entry was induced by prior store depletion in Ca^{2+}-free conditions using 1 μM Tg treatment for 3 min followed by the subsequent addition of 2 mM external Ca^{2+} (Fig. 7*A*). Around 60% of this Ca^{2+} entry is inhibited by 100 μM 2-aminoethoxydiphenyl borate and can be attributed to CCE (see *bar chart inset*). Parallel experiments were performed in MIN6 cells transiently expressing the Epac2-camps FRET sensor (Fig. 7*B*). For cAMP measurements, the AC activator, forskolin (FSK; 20 nM), and non-selective phosphodiesterase inhibitor, 3-isobutyl-1-methylxanthine (IBMX; 100 μM), were also present to potentiate cAMP production. All data are plotted as the percentage of FRET signal change relative to the maximum FRET signal that is attainable with saturating [cAMP]. Under these conditions, CCE induced an initial decrease in cAMP production (due to a reduction in AC6 activity) that was followed by a steady rise in cAMP levels. In MIN6 cells transiently transfected with AKAP150-HA, the amplitude of Ca^{2+}-stimulated cAMP production was reduced (Fig. 7, *B* and *C*). This effect was comparable with the effects of AKAP79 overexpression in HEK-AC8 cells (Fig. 3). Lentiviral shRNA directed against AKAP150 was found to reduce endogenous AKAP150 levels by around 55% (supplemental Fig. 1*B*). This knockdown of endogenous AKAP150 expression levels pro-

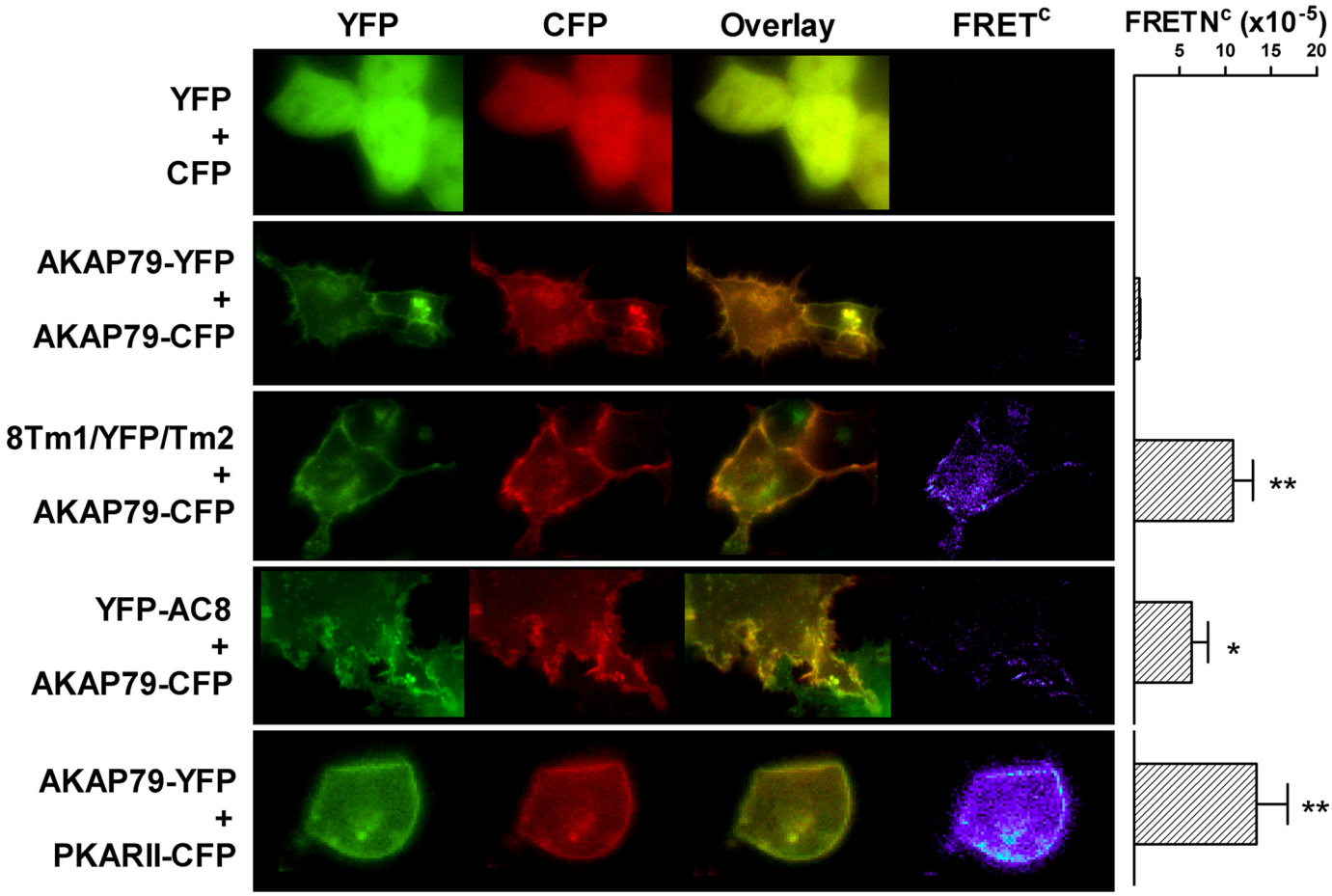

FIGURE 5. **FRET imaging of AKAP79 and AC8 interaction in live HEK293 cells.** Images of YFP-tagged (*green*) and CFP-tagged constructs (*red*) when transiently expressed in HEK293 cells. Co-localization of co-expressed constructs is shown as *yellow* in *overlay images*. The *pseudocolor images* represent FRET signals corrected for any bleed-through using the micro-FRET method ($FRET^C$). Cells co-expressing YFP + CFP or AKAP79-YFP + AKAP79-CFP showed good co-localization of fluorescent signals but no detectable $FRET^C$ signal. Co-localization (overlay) and direct interactions ($FRET^C$) between YFP-AC8 + AKAP79-CFP, 8Tm1/YFP/Tm2 + AKAP79-CFP, and PKARII-CFP + AKAP79-YFP were detected at the plasma membrane. 8Tm1/YFP/Tm2 is a truncated version of AC8 in which YFP has been inserted between residues 1 and 397 and between residues 654 and 956 (26). Normalized FRET efficiencies were calculated for all cells ($FRETN^C$; see "Experimental Procedures") and used to quantify the micro-FRET data. Each *bar* represents mean ± S.E. (*error bars*), with *n* values ranging from 9 to 12 for each FRET pair. *, $p < 0.05$; **, $p < 0.01$.

duced a marked potentiation of cAMP production compared with scrambled shRNA controls following the initial decrease in AC activity (Fig. 7*B*, *lower traces*) ($p < 0.05$). These findings further support an AKAP79/150 and AC8 interaction attenuating the stimulatory effects of Ca^{2+} on AC8 activity.

Previous studies on the distribution patterns for AC8 expression have shown that the enzyme is highly expressed within the hippocampus (31, 32), where it is believed to play an important role in memory formation (33, 34). Interestingly, the hippocampus is also a major source of AKAP79/150 expression (35–37), where it associates with a range of membrane proteins, including *N*-methyl-D-aspartate receptors (38) and L-type Ca^{2+} channels (15). Using primary cultured rat hippocampal neurons, we investigated whether a change in the expression levels of AKAP79/150 altered Ca^{2+}-stimulated AC activity. Because activity-induced changes in neuronal [Ca^{2+}] are typically accompanied by substantial local acid shifts (39), we generated a modified Epac2-camps sensor for our hippocampal experiments in which the pH-sensitive YFP (pK_a ~6.9) was replaced with citrine (pK_a ~5.8) (Fig. 8*A*), thus minimizing the potential for pH artifacts in the measured FRET signal. This new sensor, Ci/C-Epac2-camps, expressed well in ~2% of our cultured hippocampal neurons following transient transfection at 10–12 days *in vitro*. Of the neurons expressing the cAMP sensor, only pyramidal neurons (identified by cell morphology) were selected for experimental use.

In vitro calibration of the Ci/C-Epac2-camps used cell lysate from HEK293 cells transiently transfected with the new sensor and showed good sensitivity to cAMP with an estimated EC_{50} value of 210 ± 11 nM cAMP. This value fell slightly below our estimated EC_{50} of 349 ± 21 nM for the parent YFP-containing Epac2-cAMP sensor (Fig. 8*B*). Spectral analysis of the Ci/C-Epac2-camps and original Epac2-camps sensors revealed reduced pH sensitivity of the citrine compared with YFP at around 530 nm (peak emission for YFP and citrine), with the citrine showing no obvious decline in signal when switching from pH 7.3 to pH 6.7 (Fig. 8*B*, *lower plots*).

To directly examine the effects of AKAP150-HA expression on endogenous Ca^{2+}-stimulated AC activity in cultured hippocampal neurons, AC activity was compared in the absence and the presence of 2 mM external Ca^{2+}. Under control conditions, switching from 2 mM Ca^{2+} containing saline to Ca^{2+}-free saline

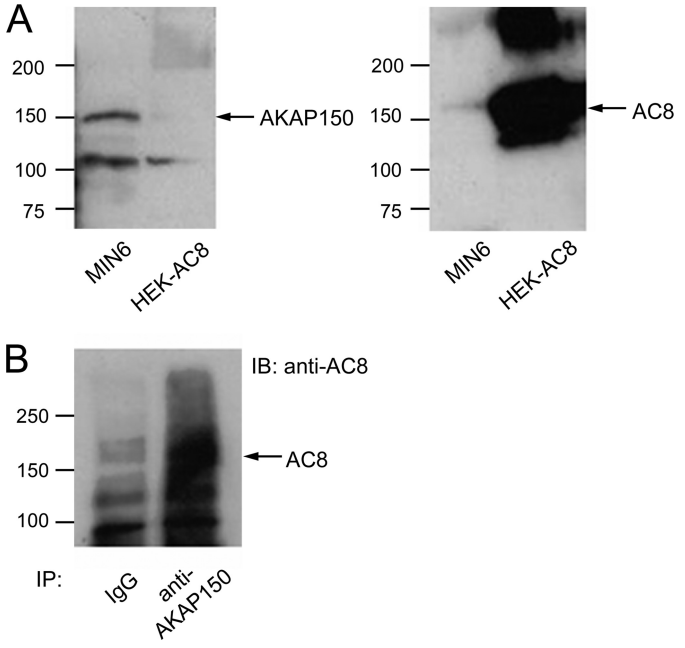

FIGURE 6. **Co-immunoprecipitation of endogenously expressed AC8 and AKAP150 in MIN6 cells.** *A*, Western blot analysis to confirm the endogenous expression of AKAP150 (*left*) and AC8 (*right*) in MIN6 cells. *B*, immune complexes for endogenous AKAP150 co-purify with AC8 in MIN6 cell lysate. No AC8 band is seen in IgG controls. Antibodies used for immunoprecipitation (*IP*) and subsequent immunoblotting (*IB*) were specific to AKAP150 and AC8, respectively.

resulted in a cessation of spontaneous Ca^{2+} transients associated with voltage-gated Ca^{2+}-channel activity (data not shown) and a notable decrease in Ci/C-Epac2-camps emission ratio, consistent with a drop in basal AC activity (Fig. 8*C*). Upon the addition of 1 μM FSK in Ca^{2+}-free conditions, cAMP levels began to rise slowly. This rate of cAMP increase was markedly potentiated upon the readdition of external Ca^{2+} at 180 s, due to stimulation of endogenous AC8 (and/or AC1) activity (Fig. 8, *C* and *D*). Maximum FRET ratio change was obtained by the subsequent addition of 10 μM FSK, 10 μM isoproterenol, and 100 μM IBMX. In parallel experiments, the transient overexpression of AKAP150-HA significantly delayed the Ca^{2+}-dependent rise in AC activity (Fig. 8, *C* and *D*). This effect of AKAP150 overexpression is again consistent with the attenuating effects of AKAP79 on AC8 activity in HEK293 cells and of AKAP150 on AC8 activity in MIN6 cells, which suggests that AKAP79/150 dampens Ca^{2+}-dependent AC8 activity as a consequence of its interaction with the enzyme. Experiments attempting to assess the effects of knockdown of endogenous AKAP150 levels proved difficult to interpret because 72–96-h lentiviral transfection with shRNA targeted against AKAP150 caused a pronounced enhancement of Ca^{2+}-insensitive AC activity in the cultured neurons (Fig. 8*C*). This enhanced rate of cAMP production was not increased further upon the addition of 2 mM Ca^{2+} to the bath solution (Fig. 8, *C* and *D*).

DISCUSSION

Despite mounting evidence for the direct association of AKAPs with Ca^{2+}-regulated ACs (5, 6), our understanding of the role of such interactions is limited. In the case of AC5/6, AKAP-targeted PKA serves to facilitate inhibition of cAMP production (5, 6); however, nothing is known regarding the effects of AKAP interaction on the highly sensitive and potentially dynamic regulation of the ACs by changes in intracellular [Ca^{2+}]. This issue is of particular interest because both the Ca^{2+}-regulated ACs and a number of specific AKAPs reside in close apposition to or direct association with sites of Ca^{2+} entry (9, 11, 15, 40, 41). Here we provide the first evidence for interaction of Ca^{2+}-stimulated AC8 with an AKAP and begin to address the function of such AKAP-AC interactions with respect to Ca^{2+}-regulated cAMP production in a range of cell types.

Direct binding between the N terminus of AC8 and AKAP79/150 was illustrated by GST pull-downs and confirmed by co-immunoprecipitation of tagged AC8 and AKAP79 constructs when overexpressed in HEK293 cells. In addition, AC8-HA associated with endogenous human AKAP79 in HEK293 cells. A protein-protein interaction was also observed between AC8 and AKAP150 (the rodent orthologue of AKAP79) in pancreatic cells endogenously expressing both protein species.

Using truncated N-terminal regions of AC8, we could narrow down the site of interaction with AKAP79/150 to residues within the first 77 amino acids of AC8. This was supported by the lack of interaction of AKAP79 with the N-terminally truncated AC8 mutant, 8M1 (Δ1–106). Our data were consistent with the hypothesis that the non-conserved N termini of ACs provide a general site of interaction during the assembly of AKAP-AC complexes (7) because the N termini of both AC2 and AC5 provided the site for interaction with Yotiao and mAKAPβ, respectively (6, 7). However, common contact sites for AKAP-AC interaction seem unlikely because mAKAPβ and AKAP79 have been shown to interact with different sites within AC5 (7). The first 77 amino acids of AC8 contain a helical calmodulin binding domain, located between residues 34 and 51 (25, 42). An overlapping region of amino acid residues is also reported to bind the protein phosphatase, protein phosphatase 2A (17). The precise residues within the N terminus of AC8 that were responsible for binding to AKAP79/150 are yet to be identified. Studies of AKAP79/150 binding to the L-type Ca^{2+} channel, Cav1.2, have identified a modified leucine zipper motif within the distal C terminus of the channel subunit that is responsible for the interaction with AKAP79/150 (15, 41, 43). We considered the possibility of a similar means of interaction of AKAP79/150 with AC8. However, sequence analysis of AC8 suggested that no such leucine zipper-like domains were present within the first 77 amino acids. Interestingly, the AKAP150 orthologue also interacted with the C2 domain of AC8 (amino acids 1106–1248) when expressed in HEK293 cells. Similar additional sites of AKAP interaction were reported for the binding of AC5 to mAKAPβ, which was found to involve all three cytosolic domains of AC5 (N terminus and C1 and C2 domains) (7).

In addition to our biochemical data, direct evidence of binding between AKAP79 and AC8 was observed using micro-FRET to confirm protein-protein interactions between AKAP79-CFP and YFP-AC8 in live cells. Switching the location of the YFP from the N terminus of AC8 to the C1 domain, as in 8Tm1/YFP/Tm2, enhanced the degree of FRET between

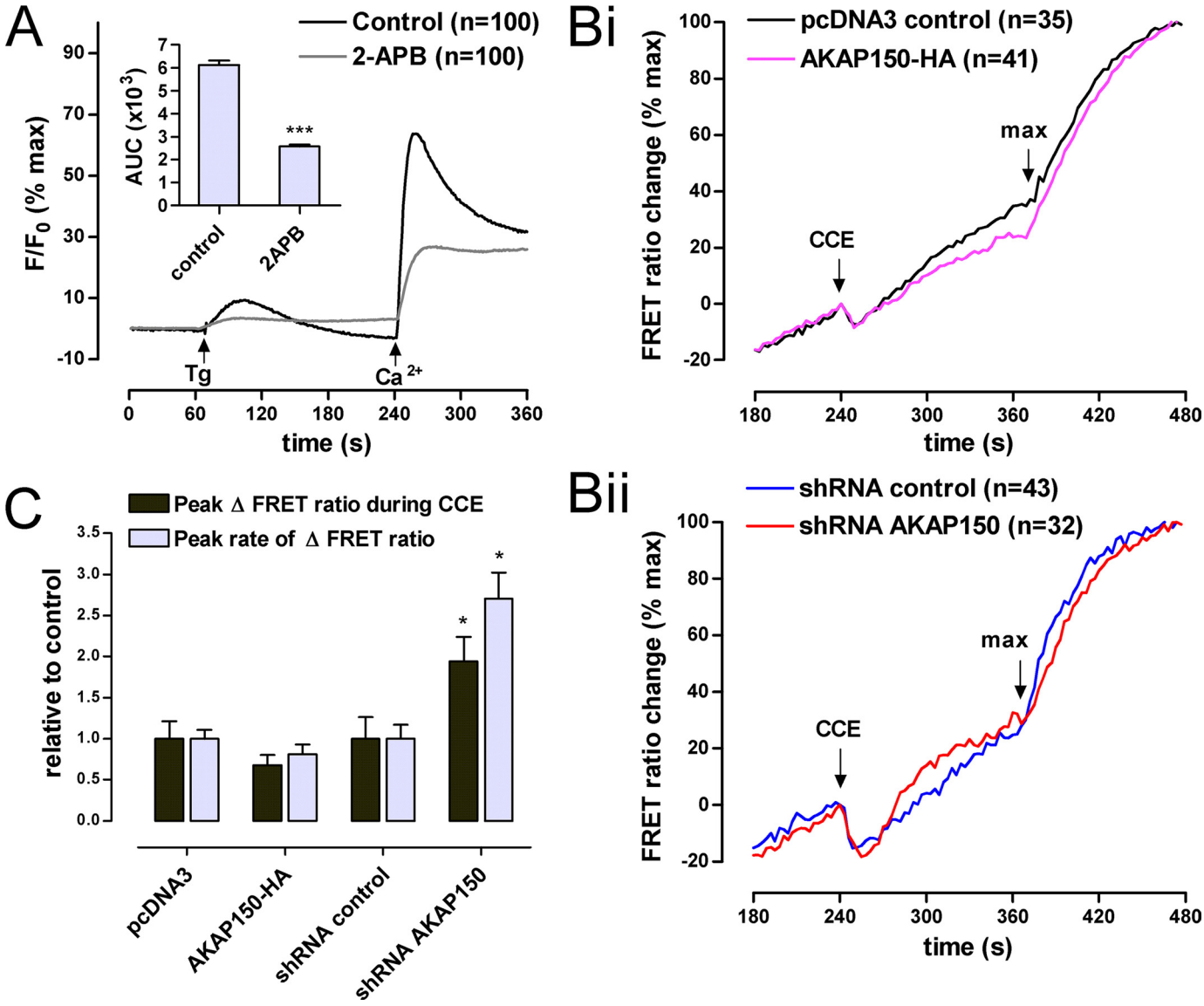

FIGURE 7. **Effects of AKAP150 on Ca^{2+}-stimulated AC8 activity in MIN6 cells.** *A*, Fura-2 data showing the standard protocol for inducing CCE in MIN6 cells. Cells were pretreated with 1 μM Tg in Ca^{2+}-free conditions for 3 min prior to the addition of 2 mM external Ca^{2+}. The addition of 100 μM 2-aminoethoxydiphenyl borate (*2-APB*; a CCE inhibitor when used at high concentrations) from 1 min onward significantly reduced Ca^{2+} entry (see *bar chart inset*; ***, $p < 0.001$). *Bi*, Epac2-camps data showing the effects of AKAP150 overexpression on Ca^{2+}-stimulated cAMP production compared with empty vector controls. 20 nM FSK and 100 μM IBMX were present throughout. Data are plotted as a percentage of maximal FRET signal obtained using saturating cAMP concentrations. *Bii*, as above, except that the effects of lentiviral shRNA directed against AKAP150 were compared with scrambled shRNA controls. *C*, *bar charts* show mean ± S.E. values (*error bars*) for peak amplitude and rate of FRET ratio changes during CCE for data in *B*. *, $p < 0.05$ compared with shRNA controls.

tagged AC8 and AKAP79 constructs. This improved FRET efficiency is likely to be mediated by subtle differences in the distance and orientation between the two fluorophores when YFP is inserted at the C1 domain of AC8. The degree of FRET observed between 8Tm1/YFP/Tm2 and AKAP79-CFP was comparable with that observed following co-expression of AKAP79-CFP with its ubiquitous binding partner PKA-RIIα (tagged to CFP).

To determine a functional role for the proposed AKAP79/150-AC8 signaling complex, Ca^{2+}-dependent AC8 activity was monitored using the FRET-based cAMP biosensor, Epac2-camps (18). In an overexpression system and when expressed endogenously, the AKAP79/150 interaction with AC8 mediated an inhibitory effect on AC8 activity. In HEK-AC8 cells, AKAP79-HA expression decreased CCE-mediated cAMP production by ~20% compared with controls, independently of any indirect effect on the amplitude of the Ca^{2+} entry signal. Because AKAP79 is endogenously expressed in HEK293 cells at relatively high levels (supplemental Fig. 1*A*), more potent modulation of the effect of AKAP79 on AC8 activity was seen when shRNA was used to selectively knock down endogenous expression of the scaffold protein. Comparable effects were also seen following disruption of AKAP-PKARII interaction (using St-Ht31). Thus, targeting of PKA to AC8 via AKAP79 might underlie the regulatory effects of AKAP79 with respect to AC8 activity. This would provide the first evidence of a regulatory effect of PKA on AC8 activity and, more specifically, an inhibitory effect of PKA on Ca^{2+}-dependent AC8 activity. We can only speculate on the precise mechanism of action for PKA. The simplest scenario would be a direct phosphorylation of

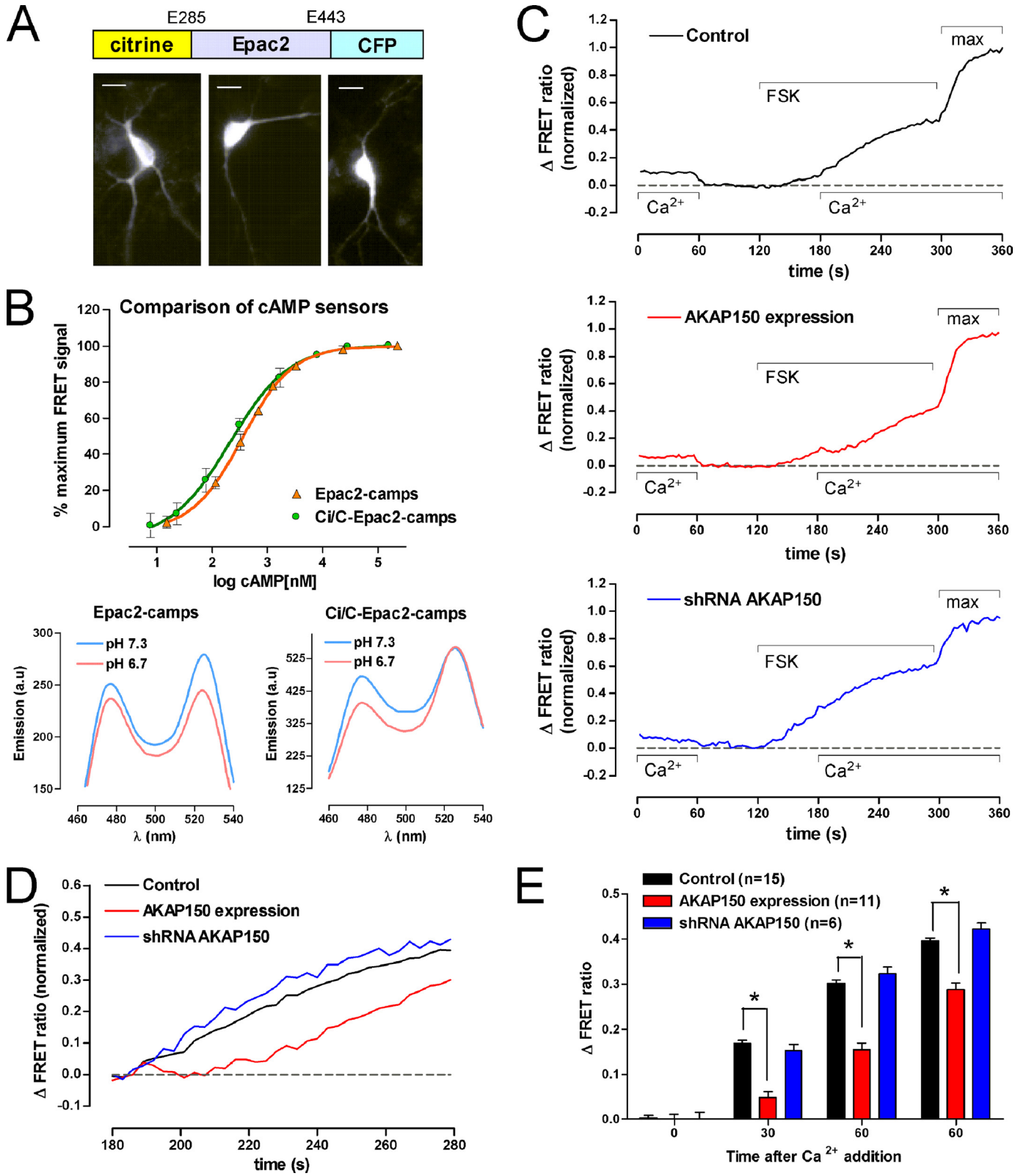

FIGURE 8. **A role for AKAP150 in the regulation of Ca^{2+}-stimulated AC activity in hippocampal neurons.** *A*, the basic design of the citrine-Epac2-camps-CFP (Ci/C-Epac2-camps) sensor used for hippocampal experiments and fluorescent images taken from three individual hippocampal neurons showing cytosolic expression of the cAMP sensor. *Scale bar*, 20 μm. *B*, *in vitro* calibrations of the Ci/C-Epac2-camps compared with the original Epac2-camps. Note the reduced pH sensitivity of the citrine-CFP version. *C*, comparison of Ca^{2+}-stimulated AC activity in control, AKAP150-HA-expressing, and AKAP150 knockdown hippocampal neurons assessed using Ci/C-Epac2-camps. 1 μM FSK was added in Ca^{2+}-free conditions at 120 s with the readdition of 2 mM external Ca^{2+} at 180 s to monitor Ca^{2+}-dependent cAMP production. Maximum FRET ratio change was obtained by the subsequent addition of 10 μM FSK, 10 μM isoproterenol, and 100 μM IBMX. *D*, overlay of control, AKAP150 overexpression, and shRNA AKAP150 data to compare Ca^{2+}-stimulated AC activities. *E*, data analysis showing significant delay in Ca^{2+} stimulation of cAMP production in neurons overexpressing AKAP150. Data represent mean ± S.E. (*error bars*) for each condition. *n* values are indicated on the *graph*. *, $p < 0.01$.

AC8 by PKA. The amino acid sequence of AC8 reveals a number of consensus PKA phosphorylation sites in the intracellular domains. An alternative mode of regulation via PKA could arise from the ability of PKA to phosphorylate and activate certain protein phosphatase 2A subunits (44). This latter option is of particular interest because protein phosphatase 2A has been shown to directly associate with the N terminus of AC8 (17). In addition, further modulatory actions of other AKAP79-associated proteins, such as protein kinase C or PP2B, cannot be discounted.

The overexpression of AKAP150-HA had opposing effects on Ca^{2+}-stimulated AC8 activity compared with AKAP79-HA, resulting in enhanced cAMP production during CCE. One possible explanation for the different effects of these two AKAP orthologues when overexpressed in HEK293 cells is the ability of the longer AKAP150 to bind to the C2 domain of AC8, in addition to the N terminus, potentially leading to competitive inhibition of any interaction of endogenous AKAP79 with AC8 in HEK293 cells. Furthermore, it is possible that the correct association of rodent AKAP150 with its typical array of signaling molecules is limited in a human cell line endogenously expressing AKAP79. Both AKAP79 and AKAP150 behaved similarly when studied in their native environments.

When we examined the role of the AKAP-AC8 interaction in physiological systems in which AKAP150 and AC8 were expressed endogenously, we saw further evidence of inhibitory regulation of AC8 activity that was dependent upon its association with AKAP150. In insulin-secreting mouse pancreatic β-cells (MIN6 cells), overexpression of AKAP150 decreased CCE-mediated AC8 activity. This effect of AKAP150 was comparable with the effects of AKAP79 in HEK-AC8 cells. However, the role of AKAP150 with respect to AC8 activity was more clearly seen when the cultured pancreatic cells were treated with a shRNA lentivirus designed to suppress endogenous expression of the AKAP. Knockdown of AKAP150 in MIN6 cells resulted in a significant increase in Ca^{2+}-stimulated AC8 activity (Fig. 7). A modest enhancement of the transient Ca^{2+}-dependent inhibition of cAMP levels was also observed. This latter effect was probably due to loss of the association of endogenous AC6 with AKAP150 that has been shown to mediate PKA inhibition of AC5/6 activity (5).

In primary cultured hippocampal pyramidal neurons, the inhibitory effects of AKAP150 on Ca^{2+}-stimulated AC activity displayed different characteristics. Overexpression of AKAP150-HA in hippocampal neurons significantly delayed Ca^{2+}-stimulated cAMP production mediated by endogenously expressed AC8 (rather than inhibiting the overall degree of AC8 activity). Bidirectional regulation of L-type Ca^{2+} channels has been reported in hippocampal neurons due to interaction of the channels with AKAP79/150 and the opposing actions of PKA and calcineurin (15). Thus, it was important to determine if the effects of AKAP150-HA expression on AC8 activity might be explained by reduced Ca^{2+} entry. Control Fura-2 experiments revealed a modest increase in basal Ca^{2+} levels and the amplitude of spontaneous Ca^{2+} transients following AKAP150 expression, but no significant difference in the amplitude or rate of Ca^{2+} entry was seen upon the readdition of external Ca^{2+} (data not shown). We therefore conclude that the inhibitory effects of AKAP150 expression on Ca^{2+}-stimulated cAMP production in hippocampal neurons were a direct consequence of an AKAP150-AC8 interaction. Previous studies have implicated essential roles for both AC8 and AKAP150 in hippocampal memory formation (33, 34, 36, 41, 45). Our evidence for a direct association between these two proteins, with a clear bifunctional consequence, has identified a potentially important site of communication between two key signaling components linked to memory formation. This is further supported by the selective targeting of AKAP79/150 and AC8 to dendritic spines (31, 35, 46, 47).

To conclude, we propose that AKAP79/150 interaction with AC8 mediates inhibition of Ca^{2+}-dependent cAMP production. Such modulated activity of AC8 is likely to have physiological significance in the pancreas and in the hippocampus in which AKAP79/150 and AC8 are co-expressed. These tissues are subject to transient fluxes in local Ca^{2+} levels that have the potential to generate localized, dynamic cAMP signals linked to important events, such as insulin secretion (12, 14) and memory formation (48, 49). The evidence presented here of the functional association of AKAP79/150 with AC8, combined with the positioning of AKAP79/150 close to sites of Ca^{2+} entry (15), could form the basis of a self-regulated multimolecular signaling complex in neurons, where the local cAMP events have the potential to regulate the activity of other AKAP79/150-associated proteins, such as PKA or L-type Ca^{2+} channels. The influence of AKAP-binding on Ca^{2+}-driven cAMP signals generated by other AC isoforms is yet to be investigated, but such a device could add a sophisticated component in tuning the interplay between Ca^{2+} and cAMP signaling.

REFERENCES

1. Wong, W., and Scott, J. D. (2004) *Nat. Rev. Mol. Cell Biol.* **5,** 959–970
2. Smith, F. D., Langeberg, L. K., and Scott, J. D. (2006) *Trends Biochem. Sci.* **31,** 316–323
3. Feliciello, A., Gottesman, M. E., and Avvedimento, E. V. (2001) *J. Mol. Biol.* **308,** 99–114
4. Michel, J. J., and Scott, J. D. (2002) *Annu. Rev. Pharmacol. Toxicol.* **42,** 235–257
5. Bauman, A. L., Soughayer, J., Nguyen, B. T., Willoughby, D., Carnegie, G. K., Wong, W., Hoshi, N., Langeberg, L. K., Cooper, D. M. F., Dessauer, C. W., and Scott, J. D. (2006) *Mol. Cell* **23,** 925–931
6. Piggott, L. A., Bauman, A. L., Scott, J. D., and Dessauer, C. W. (2008) *Proc. Natl. Acad. Sci. U.S.A.* **105,** 13835–13840
7. Kapiloff, M. S., Piggott, L. A., Sadana, R., Li, J., Heredia, L. A., Henson, E., Efendiev, R., and Dessauer, C. W. (2009) *J. Biol. Chem.* **284,** 23540–23546
8. Willoughby, D., and Cooper, D. M. F. (2007) *Physiol. Rev.* **87,** 965–1010
9. Willoughby, D., Wachten, S., Masada, N., and Cooper, D. M. F. (2010) *J. Cell Sci.* **123,** 107–117
10. Fagan, K. A., Mahey, R., and Cooper, D. M. F. (1996) *J. Biol. Chem.* **271,** 12438–12444
11. Fagan, K. A., Mons, N., and Cooper, D. M. F. (1998) *J. Biol. Chem.* **273,** 9297–9305
12. Dyachok, O., Isakov, Y., Sågetorp, J., and Tengholm, A. (2006) *Nature* **439,** 349–352
13. Willoughby, D., and Cooper, D. M. F. (2006) *J. Cell Sci.* **119,** 828–836
14. Landa, L. R., Jr., Harbeck, M., Kaihara, K., Chepurny, O., Kitiphongspattana, K., Graf, O., Nikolaev, V. O., Lohse, M. J., Holz, G. G., and Roe, M. W. (2005) *J. Biol. Chem.* **280,** 31294–31302
15. Oliveria, S. F., Dell'Acqua, M. L., and Sather, W. A. (2007) *Neuron* **55,** 261–275
16. Tu, H., Tang, T. S., Wang, Z., and Bezprozvanny, I. (2004) *J. Biol. Chem.* **279,** 19375–19382

17. Crossthwaite, A. J., Ciruela, A., Rayner, T. F., and Cooper, D. M. F. (2006) *Mol. Pharmacol.* **69,** 608–617
18. Nikolaev, V. O., Bünemann, M., Hein, L., Hannawacker, A., and Lohse, M. J. (2004) *J. Biol. Chem.* **279,** 37215–37218
19. Pertz, O., Hodgson, L., Klemke, R. L., and Hahn, K. M. (2006) *Nature* **440,** 1069–1072
20. Chen, C., and Okayama, H. (1987) *Mol. Cell. Biol.* **7,** 2745–2752
21. Belfield, J. L., Whittaker, C., Cader, M. Z., and Chawla, S. (2006) *J. Biol. Chem.* **281,** 27724–27732
22. Sorkin, A., McClure, M., Huang, F., and Carter, R. (2000) *Curr. Biol.* **10,** 1395–1398
23. Bregman, D. B., Bhattacharyya, N., and Rubin, C. S. (1989) *J. Biol. Chem.* **264,** 4648–4656
24. Carr, D. W., Stofko-Hahn, R. E., Fraser, I. D., Cone, R. D., and Scott, J. D. (1992) *J. Biol. Chem.* **267,** 16816–16823
25. Gu, C., and Cooper, D. M. F. (1999) *J. Biol. Chem.* **274,** 8012–8021
26. Gu, C., Cali, J. J., and Cooper, D. M. F. (2002) *Eur. J. Biochem.* **269,** 413–421
27. Pagano, M., Clynes, M. A., Masada, N., Ciruela, A., Ayling, L. J., Wachten, S., and Cooper, D. M. F. (2009) *Am. J. Physiol. Cell. Physiol.* **296,** C607–C619
28. Willoughby, D., Wong, W., Schaack, J., Scott, J. D., and Cooper, D. M. F. (2006) *EMBO J.* **25,** 2051–2061
29. Oliveria, S. F., Gomez, L. L., and Dell'Acqua, M. L. (2003) *J. Cell Biol.* **160,** 101–112
30. Martin, A. C., Willoughby, D., Ciruela, A., Ayling, L. J., Pagano, M., Wachten, S., Tengholm, A., and Cooper, D. M. F. (2009) *Mol. Pharmacol.* **75,** 830–842
31. Conti, A. C., Maas, J. W., Jr., Muglia, L. M., Dave, B. A., Vogt, S. K., Tran, T. T., Rayhel, E. J., and Muglia, L. J. (2007) *Neuroscience* **146,** 713–729
32. Ferguson, G. D., and Storm, D. R. (2004) *Physiology* **19,** 271–276
33. Zhang, M., Moon, C., Chan, G. C., Yang, L., Zheng, F., Conti, A. C., Muglia, L., Muglia, L. J., Storm, D. R., and Wang, H. (2008) *J. Neurosci.* **28,** 4736–4744
34. Xia, Z., and Storm, D. R. (2005) *Nat. Rev. Neurosci.* **6,** 267–276
35. Colledge, M., Dean, R. A., Scott, G. K., Langeberg, L. K., Huganir, R. L., and Scott, J. D. (2000) *Neuron* **27,** 107–119
36. Ostroveanu, A., Van der Zee, E. A., Dolga, A. M., Luiten, P. G., Eisel, U. L., and Nijholt, I. M. (2007) *Brain Res.* **1145,** 97–107
37. Génin, A., French, P., Doyère, V., Davis, S., Errington, M. L., Maroun, M., Stean, T., Truchet, B., Webber, M., Wills, T., Richter-Levin, G., Sanger, G., Hunt, S. P., Mallet, J., Laroche, S., Bliss, T. V., and O'Connor, V. (2003) *Eur. J. Neurosci.* **17,** 331–340
38. Gomez, L. L., Alam, S., Smith, K. E., Horne, E., and Dell'Acqua, M. L. (2002) *J. Neurosci.* **22,** 7027–7044
39. Willoughby, D., and Schwiening, C. J. (2002) *J. Physiol.* **544,** 487–499
40. Nakahashi, Y., Nelson, E., Fagan, K., Gonzales, E., Guillou, J. L., and Cooper, D. M. F. (1997) *J. Biol. Chem.* **272,** 18093–18097
41. Hall, D. D., Davare, M. A., Shi, M., Allen, M. L., Weisenhaus, M., McKnight, G. S., and Hell, J. W. (2007) *Biochemistry* **46,** 1635–1646
42. Simpson, R. E., Ciruela, A., and Cooper, D. M. F. (2006) *J. Biol. Chem.* **281,** 17379–17389
43. Di Biase, V., Obermair, G. J., Szabo, Z., Altier, C., Sanguesa, J., Bourinet, E., and Flucher, B. E. (2008) *J. Neurosci.* **28,** 13845–13855
44. Ahn, J. H., McAvoy, T., Rakhilin, S. V., Nishi, A., Greengard, P., and Nairn, A. C. (2007) *Proc. Natl. Acad. Sci. U.S.A.* **104,** 2979–2984
45. Tunquist, B. J., Hoshi, N., Guire, E. S., Zhang, F., Mullendorff, K., Langeberg, L. K., Raber, J., and Scott, J. D. (2008) *Proc. Natl. Acad. Sci. U.S.A.* **105,** 12557–12562
46. Smith, K. E., Gibson, E. S., and Dell'Acqua, M. L. (2006) *J. Neurosci.* **26,** 2391–2402
47. Wang, H., Pineda, V. V., Chan, G. C., Wong, S. T., Muglia, L. J., and Storm, D. R. (2003) *J. Neurosci.* **23,** 9710–9718
48. Frey, U., Huang, Y. Y., and Kandel, E. R. (1993) *Science* **260,** 1661–1664
49. Wang, H., and Storm, D. R. (2003) *Mol. Pharmacol.* **63,** 463–468